EGU2020-1492

Crystal structures and high-temperature vibrational spectra for synthetic boron and aluminum doped hydrous coesite

Yu Ye*[1], Yunfan Miao[1], Smyth R. Joseph[2], Junfeng Zhang[1].

[1]China University of Geosciences, Wuhan 430074, China; [2]University of Colorado at Boulder, 80309, CO, USA

*Correspondence: yeyu@cug.edu.cn

Abstract

Coesite, a high-pressure SiO_2 polymorph, has drawn extensive interest from the mineralogical community for a long time. In this study, we synthesized hydrous coesite samples with different B and Al concentrations at 5 and 7.5 GPa (1273 K). The B concentration could be more than 400 B/10^{6}Si with about 300 ppmw. H_2O, while the Al content can be as much as 1200 ~ 1300 Al/10^{6}Si with C_{H2O} restrained to be less than 10 ppmw. Hence, B-substitution may prefer the mechanism of $Si^{4+} = B^{3+} + H^+$, whereas Al-substitution could be dominated by $2Si^{4+} = 2Al^{3+} + O_V$. The doped B^{3+} and Al^{3+} cations may be concentrated in the Si1 and Si2 tetrahedra, respectively, and make noticeable changes in the Si-O4 and Si-O5 bond lengths. *In-situ* high-temperature Raman and Fourier Transformation Infrared (FTIR) spectra were collected at ambient pressure. The single crystals of coesite were observed to be stable up to 1500 K. The isobaric Grüneisen parameters (γ_{iP}) of the external modes (< 350 cm^{-1}) are systematically smaller in the Al-doped samples, as compared with those for the Al-free ones, while most of the OH-stretching bands shift to higher frequencies at elevated temperatures.

Experiment condition

Table 1 Starting composition and synthetic condition for each synthetic run. The B and Al element concentrations are mainly measured by fs-LA-ICP-MAS, while the H Contents are estimated by FTIR

Run No.	Starting materials (wt.%)	Pressure (Gpa)	Temperature(°C)	Time (hr.)	B (ppmw.)	B/10^{6}Si	Al (ppmw.)	Al/10^{6}Si	H_2O (ppmw.)	H/10^{6}Si
R503	SiO_2 + 1μL H_2O	7.5	1000	12	—	—	—	—	32.3±14.2	215±95
R663	SiO_2 (96) + H_3BO_3 (4) + 1μL H_2O	5	1000	10	74.6±3.5	445±21	—	—	51.0±19.8	340±132
R694	SiO_2 (94) + H_3BO_3 (3) + $Al(OH)_3$ (3) + 1μL H_2O	5	1000	10	73.4±9.0	437±54	115.6±52.0	343±154	22.8±11.7	152±78
R712	SiO_2 (94) + H_3BO_3 (3) + $Al(OH)_3$ (3) + 1μL H_2O	7.5	1000	9	39.7±8.2	237±49	139.8±31.7	415±94	24.1±10.9	161±73
R749	SiO_2 (96) + $Al(OH)_3$ (4) + 1μL H_2O	5	1000	9	—	—	445.8±86.5	1323±257	7.2±2.9	48±19

Hydration and B/Al concentrations

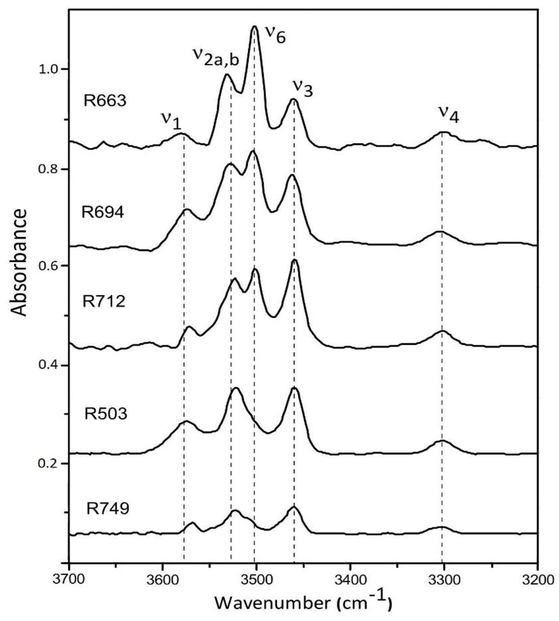

The representative FTIR spectra for these synthetic coesite samples at ambient condition are shown in **Fig. 1.** The hydration concentrations in these synthetic samples show a general trend: R663 (B-doped) > R503 (B,Al-free) > R694 / R712 (B,Al-doped) > R749 (Al-doped). This observation can be interpreted as results of different incorporation mechanisms between B and Al in coesite. The predominant B-substitution mechanism in coesite should be an electrostatically coupled substitution $Si^{4+} = B^{3+} + H^+$,which could increase hydration solubility, as compared with the Si-pure sample R503. In contrast, most of Al cations were incorporated into the internal structure of coesite by causing oxygen vacancies ($2Si^{4+} = 2Al^{3+} + O_V$), such Al-corporation may have an effect of reducing water solubility in coesite, according to the estimated water content in the sample R749.

Figure 1. *Representative FTIR spectra obtained at ambient conditions with the OH-stretching bands noted.*

Crystal structures

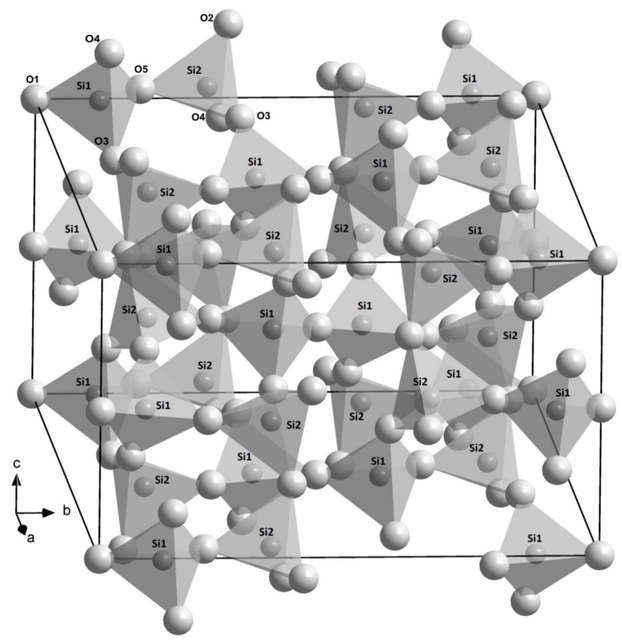

Figure 2. *Crystal structure of coesite sketched on the basis of the structure refinement for the sample R503 in this study. The smaller and larger balls represent Si and O atoms.*

The space group of coesite is *C*2/*c*, and SiO_4 tetrahedra form an infinite 3-dimensional framework of a (*b*-unique) monoclinic structure(**Fig. 2**). There are totally two Si sites and five O sites in the lattice. The measured unit-cell volumes of the B-doped (R663), B,Al-doped (R694 and R712) and Al-doped (R749) samples differ -0.15 %, -0.3 ~ -0.4 %, and +0.1 %, away from that for the Si-pure one (R503), respectively, while such differences are significantly larger than the experimental uncertainty from single-crystal XRD. Hence, even a few hundred ppm concentrations of B and Al trace elements could have noticeable impact on the volume of coesite.

Lattice vibrations and Grüneisen parameters

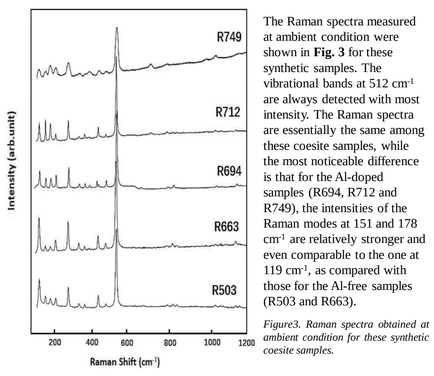

The Raman spectra measured at ambient condition were shown in **Fig. 3** for these synthetic samples. The vibrational bands at 512 cm^{-1} are always detected with most intensity. The Raman spectra are essentially the same among these coesite samples, while the most noticeable difference is that for the Al-doped samples (R694, R712 and R749), the intensities of the Raman modes at 151 and 178 cm^{-1} are relatively stronger and even comparable to the one at 119 cm^{-1}, as compared with those for the Al-free samples (R503 and R663).

Figure3. Raman spectra obtained at ambient condition for these synthetic coesite samples.

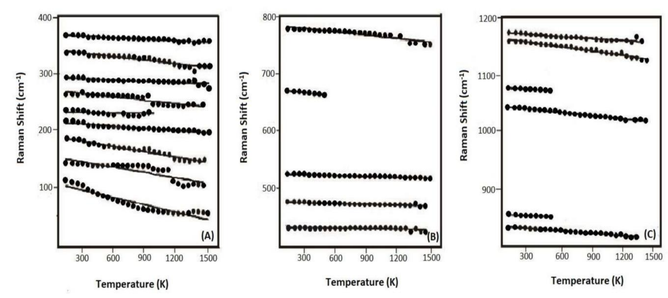

Figure 5. *Variation of the frequencies for the Raman-active modes (R503) with temperature, in the frequency ranges of* ***(A)*** *0 - 400 cm^{-1},* ***(B)*** *400 - 800 cm^{-1} and* ***(C)*** *800 - 1200 cm^{-1}. Linear regression is fitted for each dataset.*

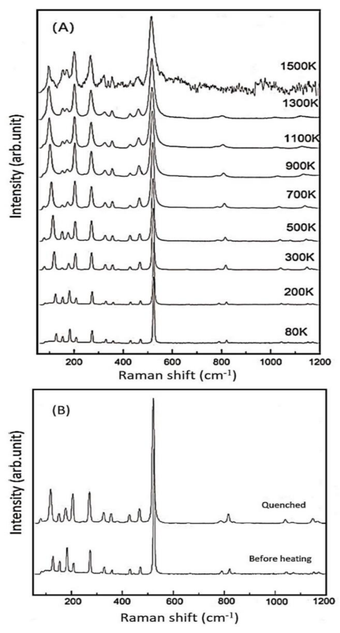

Figure 4. (A) *Selected Raman spectra for the sample of R503 at various temperatures; (B) comparison of the Raman spectra taken before and after heating.*

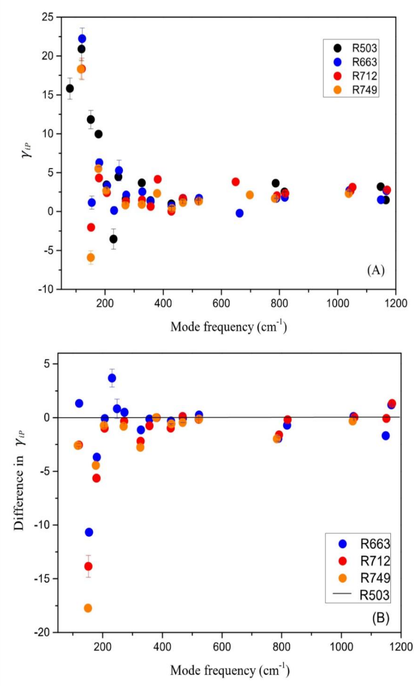

The differences of the γ_{iP} parameters among the samples of R663, R712, R749 and R503 (reference) are plotted in **Fig. 6(B)**.The most significant difference is that in the frequency range below 350 cm^{-1}, the g_{iP} parameters for the Al-doped samples (R712 and R749) are systematically lower than those for the Al-free ones (R503 and R663), while no such differences are observed above 400 cm^{-1}. When the Al^{3+} cations take place of Si^{4+} in the tetrahedra, the thermal response of the enlarged tetrahedra units could get hindered to some extent at high temperature, while the smaller B^{3+} cations do not such effect on the external vibrations of the tetrahedra units in coesite.

Figure 6. (A) *The isobaric mode Grüneisen parameters (g_{iP}) for the synthetic samples of R503, R663, R712 and R749; (B) Comparison among the g_{iP} parameters with the ones for the sample R503 set as reference.*

OH-stretching modes at high temperature

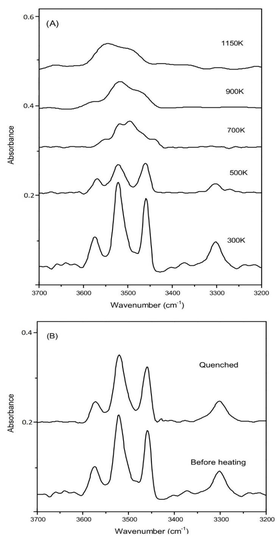

The selected high-temperature FTIR spectra for R503 are shown in **Fig. 7(A)** in the temperature range up to 1150 K. The IR signal weakers at higher temperature, and the OH-stretching modes of ν_1, $\nu_{2a,b}$ and ν_3 (in the frequency range of 3450 ~ 3600 cm^{-1}) merge to be a broad hump above 700 K. The weak and discrete ν_4 band (around 3300 cm^{-1}) vanishes very quickly, and cannot be detected above 500 K.

Another FTIR spectrum was collected when quenched to room temperature, and all these four OH-stretching bands could be clearly identified at the same positions as before heating(**Fig.7B**). The integrated absorbance for all these OH modes is about 80 % of that before heating, and then 20 % of the OH groups in the sample could be dehydrated during the heating procedure up to 1150 K.

Figure 7. (A) Representative spectra for the sample of R503 at elevated temperatures; (B) comparison of the OH-stretching bands measured before and after heating.

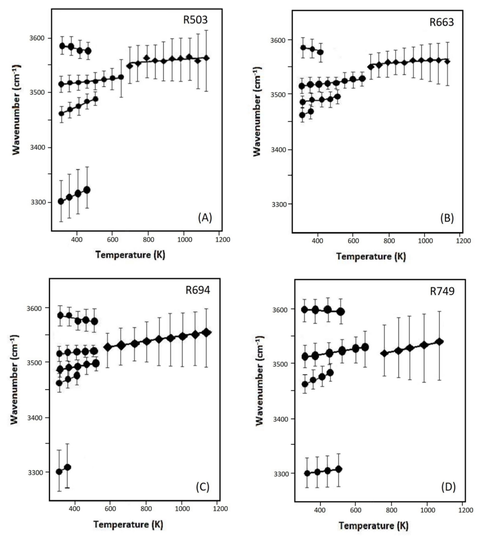

Variations of the OH bands with temperature are plotted in **Fig. 8(A-D)** for samples R503, R663, R694 and R749. At elevated temperature, the modes of $\nu_{2a,b}$, ν_3, as well as ν_6 (for B-doped samples of R663 and R712) were observed to show 'blue-shift' with a slope ($\delta\nu_i/\delta T$) of +0.03 ~ +0.05 cm$^{-1}\cdot$K^{-1}, whereas a slight 'red shift' is detected for the ν_1 mode (at the high frequency around 3600 cm^{-1}) with a temperature derivative of -0.01 ~ -0.02 cm$^{-1}\cdot$K^{-1}. Above 600 ~ 700 K, these OH vibrations cannot be distinguished from each other, and the broad hump is observed to gradually move to higher frequency at higher temperature, with a temperature dependence of +0.02 ~ +0.04 cm$^{-1}\cdot$K^{-1}. In addition, the ν_4 mode also shows 'blue shift' with temperature increasing below 500 K.

Figure 8. The frequencies of the OH-stretching modes as a function of temperature for the samples of (A) R503, (B) R663, (C) R694 and (D) R749. Linear regression lines are fitted, and the vertical error bars represent the full-width of half maximum for each OH-stretching mode.

Conclusion

1) We synthesized coesite samples with different B and Al compositions. The B concentrations are more than 400 atomic ppm (B/10^{6}Si) with ~ 350 ppmw. H_2O, while the Al^{3+} contents are 1100 ~ 1300 atomic ppm. Al-substitution significantly reduces the hydrogen concentration in coesite. Hence, the mechanism controlled by oxygen vacancies ($2Si^{4+} = 2Al^{3+} + O_V$) may be dominant for the Al incorporation, while the B incorporation may prefer the electrostatically coupled substitution ($Si^{4+} = B^{3+} + H^+$).
2) The doped B^{3+} and Al^{3+} cations would prefer the Si1 and Si2 tetrahedra , and the single-crystal structure refinements reveal that B^{3+} significantly shortens the Si1-O4 and Si1-O5 bond lengths whereas Al^{3+} noticeably elongates the Si2-O4 and Si2-O5 distances.
3) The derived isobaric mode Grüneisen parameters (γ_{iP}) for the external vibrations of SiO_4 units are significantly reduced for the Al-doped samples, as compared with the Al-free ones. Hence, the relaxation of the SiO_4 units might be hindered to some extent due to the enlarged tetrahedra units by Al-substitution. On the other hand, the γ_{iP} parameters for the internal bending and stretching modes of SiO_4 tetrahedra in coesite are significantly larger than those of most silicate minerals, due to the abnormally small thermal expansion coefficient for coesite.
4) Most of the OH vibrational modes shift to higher frequencies at elevated temperatures, implying that the O...O distances between different SiO_4 gets longer during the thermal relaxation of the lattice framework at high temperature. About 20 ~ 40 % dehydration of OH groups were observed for these coesite samples at high temperatures above 1000 K at ambient pressure.

References

1. Gillet. P.; Le, C.A.; Madon, M. High-temperature Raman spectroscopy of SiO_2 and GeO_2 polymorphs: anharmonicity and thermodynamic properties at high-temperatures. *J. Geophys. Res.* **1990**, *95(B13)*, 21635-21655.
2. Koch-Müller, M.; Fei, Y.; Hauri, E. Location and quantitative analysis of OH in coesite. *Phys. Chem. Miner.* **2001**. *28*, 693-705.
3. Smyth, J.R.; Hatton, C.J. A coesite-sanidine grospydite from the Roberts-Victor Kimberlite. *Earth Planet. Sci. Lett.* **1977**, *34*, 284-290.
4. Wang, X.; Xu, X.; Ye, Y.; Wang, C.; Liu, D.; Shi, X.; Wang, S.; Zhu, X. *In-situ* high-temperature XRD and FTIR for calcite, dolomite and magnesite: anharmonic contribution to the thermodynamic properties. *J. Earth Sci.* **2019**, *30*, 964-976.
5. Williams, Q.; Hemley, R.L.; Kruger, M.B.; Jeanloz, R. High pressure infrared spectra of α-quartz, coesite, stishovite and silica glass. *J. Geophys. Res.* **1993**, *98*, 157-170.